Received: 21 September 2022 | Revised: 24 November 2022 | Accepted: 23 December 2022

DOI: 10.1002/mp.16215

RESEARCH ARTICLE

MEDICAL PHYSICS

Use of a neural network-based prediction method to calculate the therapeutic dose in boron neutron capture therapy of patients with glioblastoma

Feng Tian[1] | **Sheng Zhao**[1] | **Changran Geng**[1,2] | **Chang Guo**[3] | **Renyao Wu**[1] | **Xiaobin Tang**[1,2]

[1]Department of Nuclear Science and Technology, Nanjing University of Aeronautics and Astronautics, Nanjing, People's Republic of China

[2]Joint International Research Laboratory on Advanced Particle Therapy, Nanjing University of Aeronautics and Astronautics, Nanjing, People's Republic of China

[3]Department of Radiation Oncology, Jiangsu Cancer Hospital, Nanjing, People's Republic of China

Correspondence
Changran Geng and Xiaobin Tang, Department of Nuclear Science and Technology, Nanjing University of Aeronautics and Astronautics, Nanjing, 210016, People's Republic of China.
Email: gengchr@nuaa.edu.cn and tangxiaobin@nuaa.edu.cn

Funding information
National Key Research and Development Program, Grant/Award Number: 2022YFE0107800; National Natural Science Foundation of China, Grant/Award Number: 12220101005; Natural Science Foundation of Jiangsu Province, Grant/Award Number: BK20220132; Fundamental Research Funds for the Central Universities, Grant/Award Number: NG2022004

Abstract

Background: Boron neutron capture therapy (BNCT) is a binary radiotherapy based on the $^{10}B(n, \alpha)^{7}Li$ capture reaction. Nonradioactive isotope ^{10}B atoms which selectively concentrated in tumor cells will react with low energy neutrons (mainly thermal neutrons) to produce secondary particles with high linear energy transfer, thus depositing dose in tumor cells. In clinical practice, an appropriate treatment plan needs to be set on the basis of the treatment planning system (TPS). Existing BNCT TPSs usually use the Monte Carlo method to determine the three-dimensional (3D) therapeutic dose distribution, which often requires a lot of calculation time due to the complexity of simulating neutron transportation.

Purpose: A neural network-based BNCT dose prediction method is proposed to achieve the rapid and accurate acquisition of BNCT 3D therapeutic dose distribution for patients with glioblastoma to solve the time-consuming problem of BNCT dose calculation in clinic.

Methods: The clinical data of 122 patients with glioblastoma are collected. Eighteen patients are used as a test set, and the rest are used as a training set. The 3D-UNET is constructed through the design optimization of input and output data sets based on radiation field information and patient CT information to enable the prediction of 3D dose distribution of BNCT.

Results: The average mean absolute error of the predicted and simulated equivalent doses of each organ are all less than 1 Gy. For the dose to 95% of the GTV volume (D_{95}), the relative deviation between predicted and simulated results are all less than 2%. The average 2 mm/2% gamma index is 89.67%, and the average 3 mm/3% gamma index is 96.78%. The calculation takes about 6 h to simulate the 3D therapeutic dose distribution of a patient with glioblastoma by Monte Carlo method using Intel Xeon E5-2699 v4, whereas the time required by the method proposed in this study is almost less than 1 s using a Titan-V graphics card.

Conclusions: This study proposes a 3D dose prediction method based on 3D-UNET architecture in BNCT, and the feasibility of this method is demonstrated. Results indicate that the method can remarkably reduce the time required for calculation and ensure the accuracy of the predicted 3D therapeutic dose-effect. This work is expected to promote the clinical development of BNCT in the future.

KEYWORDS
3D therapeutic dose, 3D-UNET, boron neutron capture therapy, neural network

Feng Tian and Sheng Zhao contributed equally to this work.

1 | INTRODUCTION

Boron neutron capture therapy (BNCT) is a binary radiotherapy based on the $^{10}B(n,\alpha)^{7}Li$ capture reaction, which releases two charged particles (i.e., α and ^{7}Li) with high linear energy transfer.[1,2] In previous decades and recently, BNCT has raised much interest because of its targeted treatment, low toxicity, and high efficiency, and many countries, such as in Japan,[3] in Europe,[4,5] and recently in China,[6] have vigorously developed the BNCT technology. Given its high biological effectiveness, BNCT has unique advantages in the treatment of recurrent head and neck malignancies, glioblastoma, and melanomas, and the therapeutic effect has been demonstrated in some existing clinical cases.[7–9]

An accurate BNCT treatment plan is the key to guiding the actual treatment.[10] Considering the complexity of neutron transport, current BNCT treatment planning systems (BNCT-TPSs) for example, NCT_Plan,[11] simulation environment for radiotherapy applications (SERA),[12] THORplan,[13] NeuCure system,[14] and JAEA computational dosimetry system,[15] all use the Monte Carlo (MC) method to evaluate the therapeutic dose.[16] Although it can achieve satisfactory three-dimensional (3D) therapeutic dose calculations, the MC method is often time-consuming,[17] that is, takes several hours. Recently, the neural network (NN) technology has been applied in various fields of medicine, such as medical image segmentation, automated radiation therapy treatment planning, dose prediction.[18,19] A NN is a series of algorithms that endeavors to recognize underlying relationships in a set of data through a process that mimics the way the human brain operates.[20] It will adjust its own parameters to establish the mapping relationship between input data and target data. In the field of conventional photon radiotherapy, the feasibility of obtaining the 3D dose distribution of patients with malignant tumors, such as head and neck, prostate, breast, and lung cancers, based on NN has been demonstrated.[21] Related research also showed that the use of NN can reduce the time required for dose calculations.[22] The successful application of NN in the field of photon radiotherapy provides ideas and confidence for its application in other fields of radiotherapy. R. Ahangari et al. has proposed to use the artificial neural network to predicted the one-dimensional dose distribution in Snyder head phantom so as to evaluate the quality of neutron beam.[23] However, to our knowledge, no study on NN-based patient dose prediction has been performed in BNCT, which is far more complex and time-consuming than photon and charged-particle therapies.

In this paper, a NN-based method for the rapid assessment of the 3D therapeutic dose distribution of patients with glioblastoma in BNCT is proposed, and the feasibility of this method is demonstrated through dose volume histograms (DVH), gamma index, dose deviation analysis, and other methods.

2 | MATERIALS AND METHODS

2.1 | Patient data and preprocessing

In this study, we collect CT data from 122 patients (male: 78, female: 44) with glioblastoma at the Jiangsu Cancer Hospital from March 2021 to March 2022. Their ages range from 29 years to 81 years, and the median age of all patients is 58 years. All data have been authorized by the Ethics Committee of Jiangsu Cancer Hospital (ID: 2022011). Radiation oncologists have delineated the gross tumor volume (GTV), skin, and organs at risk (OAR) in the planning CT. The dimension of CT images is ranged to $125 \times 125 \times 60$, and the corresponding pixel size is $2.5391 \times 2.5391 \times 3$ mm^3. A total of 104 cases are used as training set, and 18 cases are used as test set. The organs and organ numbers involved in this work are shown in Table 1.

2.2 | Configuration of 3D U-NET

In this work, the 3D BNCT therapeutic dose distribution is predicted through 3D-UNET[24,25] as shown in Figure 1. The encoder creates multi-level, multi-resolution feature representations by computing feature maps of various sizes and degrees of abstraction from the input patches of 3D images. Instead of directly performing supervision and loss back propagation on the high-level semantic features, the decoder decodes the features. The skip connection ensures that the final recovered feature map contains more low-level features. Additionally, dimensional features allow for the fusion of features at various scales.[26]

The encoder is a Visual Geometry Group (VGG-style)[27] convolutional neural network consisting of two convolutional modules, each followed by a leaky rectified

TABLE 1 Organs involved in this work

Organ	Organ label
GTV	1
Brain stem	2
Eye (left/right)	3/4
Optic nerve (left/right)	5/6
Skull	7
Brain	8
Skin	9

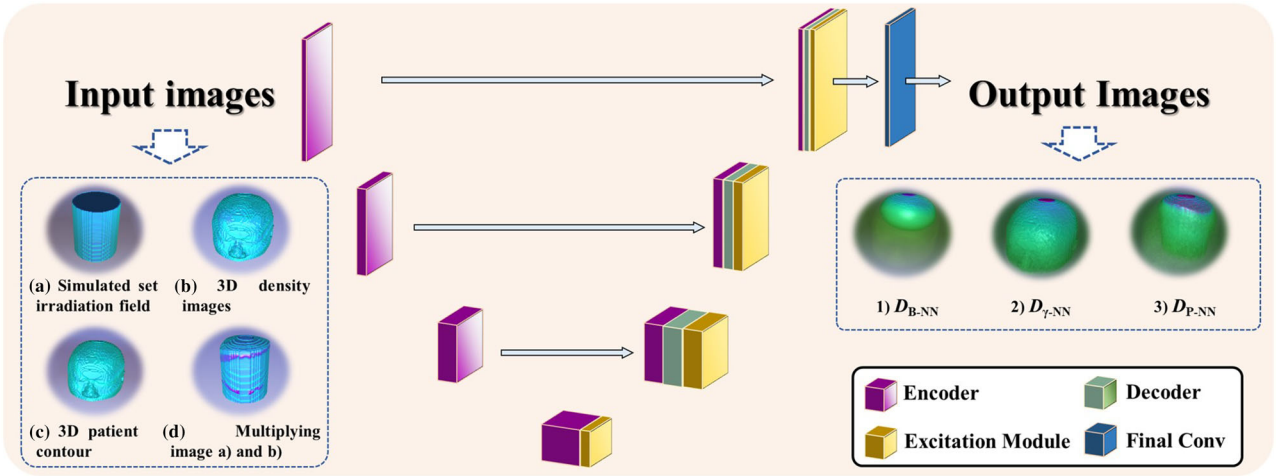

FIGURE 1 Configuration of 3D U-NET used in this study.

linear unit (LeakyReLU)[28] with a leaky factor of 0.1 and a max pooling operation with a stride of 2. The decoder restores and decodes the abstract features to the size of the original image by transposing the convolution and then connects with the cropped encoder feature map. Each convolution is followed by a leakage factor of 0.1 LeakyReLU. The 3D dose distribution for BNCT is output through the final convolutional layer.

The 3D-UNET is designed with four 3D-matrices as input, that is, ① 3D density image; ② 3D irradiation field; ③ 3D patient contour; ④ a 3D image calculated by multiplying image ① and ②. For the 3D irradiation field matrix, voxels within the irradiation field are assigned a value of 1, and those outside the irradiation field are given a value of 0. In the same way, in patient contour images, voxels inside of patients are given a value of 1, and those outside of patients are given a value of 0. The 3D therapeutic dose for BNCT consists of four parts, that is, boron dose (^{10}B(n, α)^{7}Li), fast neutron dose (^{1}H(n, n')^{1}H), thermal neutron dose (^{14}N(n, p)^{14}C), and gamma dose. Since fast neutron dose and thermal neutron dose are all caused by the protons and share the same relative biological effectiveness (RBE) factors, these two dose distributions are added and the result is named as proton dose in this study. Therefore, when analyzing the 3D therapeutic dose of BNCT, three dose components are analyzed, that is, boron dose (D_B); proton dose (D_p); and gamma dose (D_γ). The photon-equivalent dose (D) is obtained by multiplying the doses of the different components and the corresponding RBE or compound biological effectiveness (CBE), as shown in equation (1). In this current paper, all the doses presented in the results are RBE or CBE weighted doses with the unit of Gy. The parameter W_B is the corresponding CBE factor of D_B. When using the amino acid *p*-boronophenylalanine (BPA), W_B is 3.8 for tumor; 1.4 for normal organs and 2.5 for skin.[29] The parameter W_p is the corresponding the RBE factors of D_p, and for all tissues, W_p is 3.2.

$$D = W_B \times D_B + W_p \times D_p + D_\gamma \quad (1)$$

Therefore, we train three separate networks to estimate the boron dose per ppm boron-10 ($D_{B\text{-}NN}$), gamma RBE-dose ($D_{\gamma\text{-}NN}$), and proton RBE-dose ($D_{P\text{-}NN}$) which represents $W_p \times D_p$ in equation (1), respectively. The equivalent dose predicted by NN (D_{NN}) can be obtained as equation (2). The parameter C_B in equation (2) is the boron concentration distribution of the patient, which is often obtained by in vitro experiments or PET scanning.[30,31]

$$D_{NN} = W_B \times C_B \times D_{B-NN} + D_{P-NN} + D_{\gamma-NN}. \quad (2)$$

2.3 | Monte Carlo simulation and dose calculation

The Geant4 MC toolkit is used to perform the coupled simulation for neutrons, charged particles, and photons. The number of simulated particles for each patient is 2×10^8 to ensure enough uncertainties as in previous studies.[32] The doses calculated in this study are all 30-min RBE doses. The boron concentrations of the tumor, normal tissues, and skin are set as 60, 18, and 25 ppm,[33,34] respectively. The TOP irradiation geometry (i.e., the neutrons irradiating from head to foot) is used, as shown in Figure 2a. In simulations, the airgap between the neutron source and the surface of the patient with glioblastoma is 10 cm. The diameter of the incident neutron beam set in the simulations is 12 cm, and the center of incident neutron beam corresponds to the center of the tumor. The Massachusetts Institute

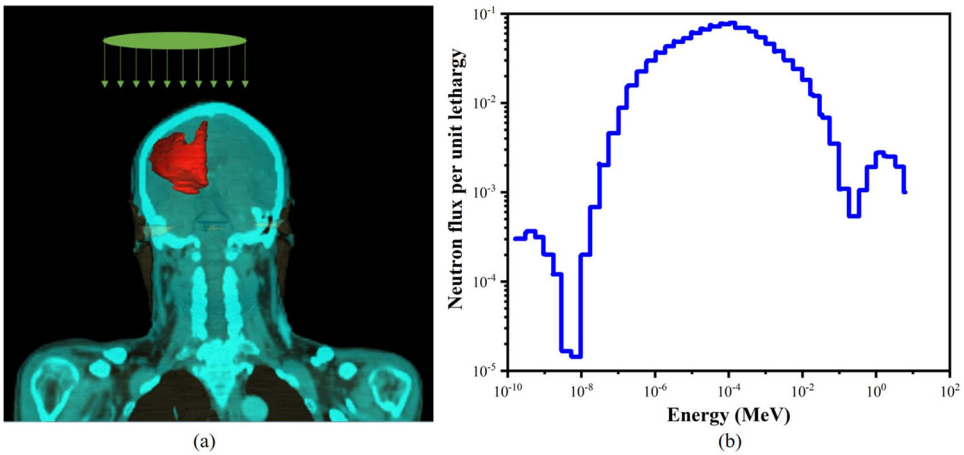

FIGURE 2 (a) Head glioblastoma location and irradiation geometries. (b) Incident neutron spectrum used in the simulations.

of Technology reactor neutron source is selected, and the energy spectrum is shown in Figure 2b.[35,36] The equivalent dose obtained for different tissues by the MC method (D_{MC}) is calculated by the counting card combined with the kerma factor.[37]

2.4 | Prediction performance evaluation

In this study, the prediction performance of the 3D-UNET is assessed in two ways. The first direct way is to evaluate the dose deviation (D_{dev}), and relative deviation (R_{dev}) between D_{MC} and D_{NN} for each voxel, as shown in equations (3) and (4), respectively. The mean absolute errors (MAE) of different organs are also calculated, as shown in equation (5), where i stands for voxel point, and n is the total voxel of different organ.

$$D_{dev} = D_{NN} - D_{MC}. \tag{3}$$

$$R_{dev} = \frac{|D_{NN} - D_{MC}|}{D_{MC}}. \tag{4}$$

$$MAE = \frac{\sum_{i=1}^{n} \left| D_{NN_i} - D_{MC_i} \right|}{n}. \tag{5}$$

The DVH comparison between simulated and predicted results are presented, and the relative deviation results of doses received by 99% (D_{99}), 98% (D_{98}), 95% (D_{95}), 50% (D_{50}), and 2% (D_2) of the GTVs' volume of all patients are calculated to assess the performance of this 3D dose prediction method. The gamma index is also calculated to assess the prediction results, and only the voxels whose dose value is higher than 10% of the maximum dose are counted.[38]

3 | RESULTS

3.1 | Prediction results of 3D therapeutic dose distribution

On the basis of the data processing method and 3D U-NET network described above, we complete the training and prediction of the BNCT 3D therapeutic dose. Loss function results of the different dose components at 250 epochs are shown in Figure S1, where the number of epoch indicates the number times that the NN will work through the entire training set.[39] According to the value of loss function, the 249th epoch is selected to predict the BNCT therapeutic dose. Taking the result of a patient with glioblastoma as an example, D_{NN} and D_{MC} are shown in Figure 3. From top to bottom, Figure 3 shows the organ and dose distribution results of the 8th, 12th, and 22nd layers of this patient. Results show that the 3D therapeutic dose distribution of patients can be well predicted on the basis of the 3D U-NET network, input and output data designed in this work. In addition to the results shown in this paper, we also present the 3D dose results of other patients in Figures S2-S5.

The relative deviation of therapeutic dose of different organs in the test data are also analyzed. The relative deviation can be calculated using equation (3), the therapeutic results are shown in Figure 4 and Table 2. The average deviation of skin dose predicted could reach 10%, and that of other organs, including GTV, is about 2%–4%. However, MAE results show that the average MAE of all organs are less than 1 Gy. Further, the maximum dose (D_{max}), average dose (D_{mean}), and minimum dose (D_{min}) of different organs in 18 patients are calculated, as shown in Table 3. It can be seen that the D_{NN} values of different organs are close to D_{MC}, which further demonstrates the accuracy of the dose prediction method proposed in this work.

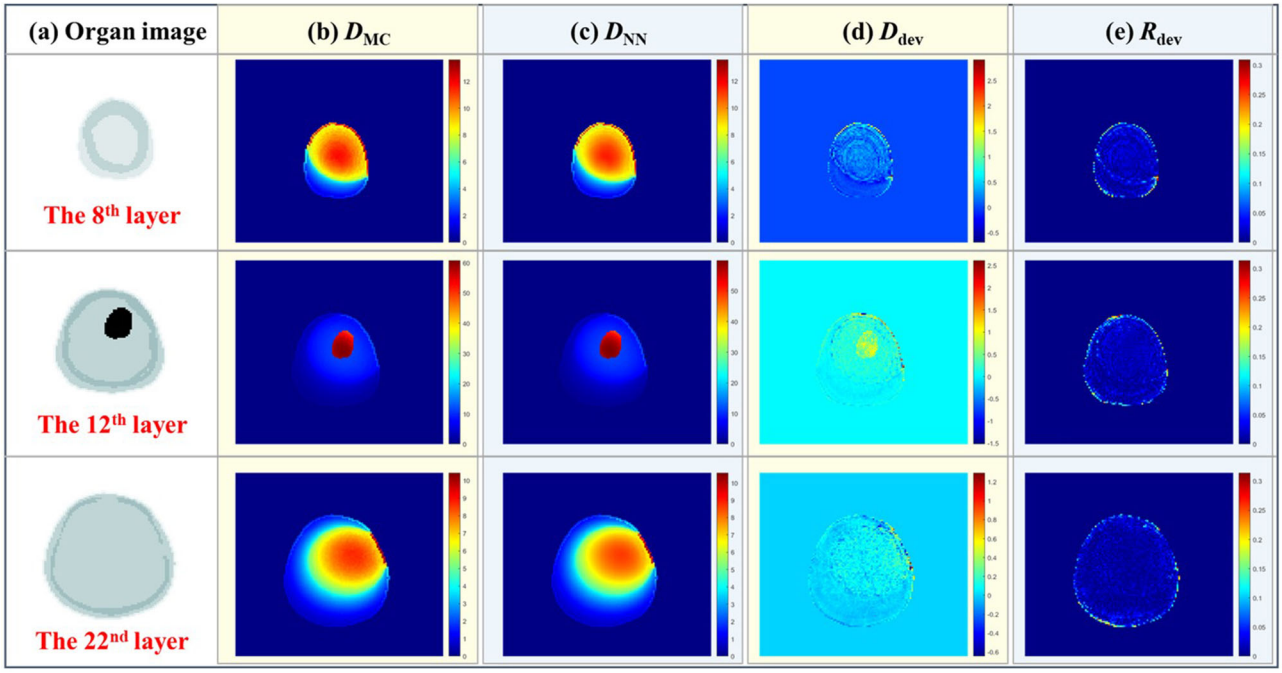

FIGURE 3 Comparison of simulated and predicted dose distributions in different depths. (a) Organ distribution map at different depths. (b) The distribution of D_{MC} at different depths. (c) The distribution of D_{NN} at different depths. (d) Deviation distribution at different depths between D_{MC} and D_{NN}. (e) Relative deviation at different depths between D_{MC} and D_{NN}.

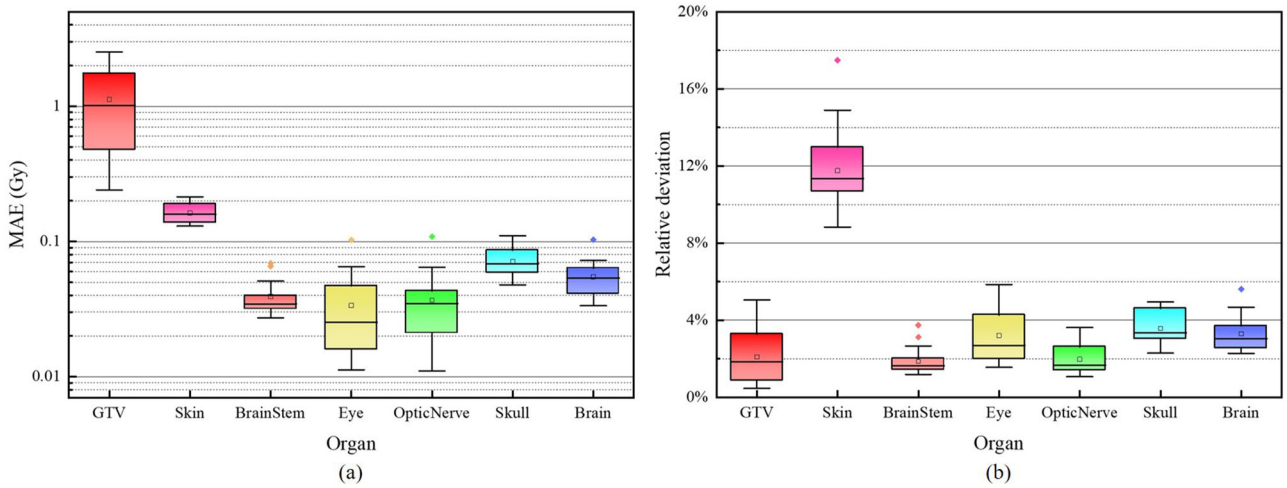

FIGURE 4 Deviation results of D_{NN} and D_{MC} of different organs. (a) MAE between D_{NN} and D_{MC} of different organs. (b) Relative deviation between D_{NN} and D_{MC} of different organs.

Further, the prediction effects of the three dose components have been evaluated, respectively. The MAE and relative deviation of different dose components of different organs in the test data are shown in Figure 5. It should be noted that the boron dose presented in Figure 5 is the REB boron dose calculated by equation (2) (i.e., $W_B \times C_B \times D_{B\text{-}NN}$), the proton dose is $D_{P\text{-}NN}$ and the gamma dose is $D_{\gamma\text{-}NN}$. It can be seen that the predicted results of the three dose components are very close to the simulation results. The MAE of GTV is the largest in all organs. For boron dose, the average MAE of GTV is about 1 Gy, while for the other two dose components, the average MAE of GTV is almost less than 0.1 Gy. In addition, it can be seen from the relative deviation results that the mean relative deviation of skin is the largest in all organs, especially the boron dose and proton dose.

The reason for this phenomenon could be that the region of skin is the edge of the patient and dose distribution, and most skin pixels receive low doses. In order

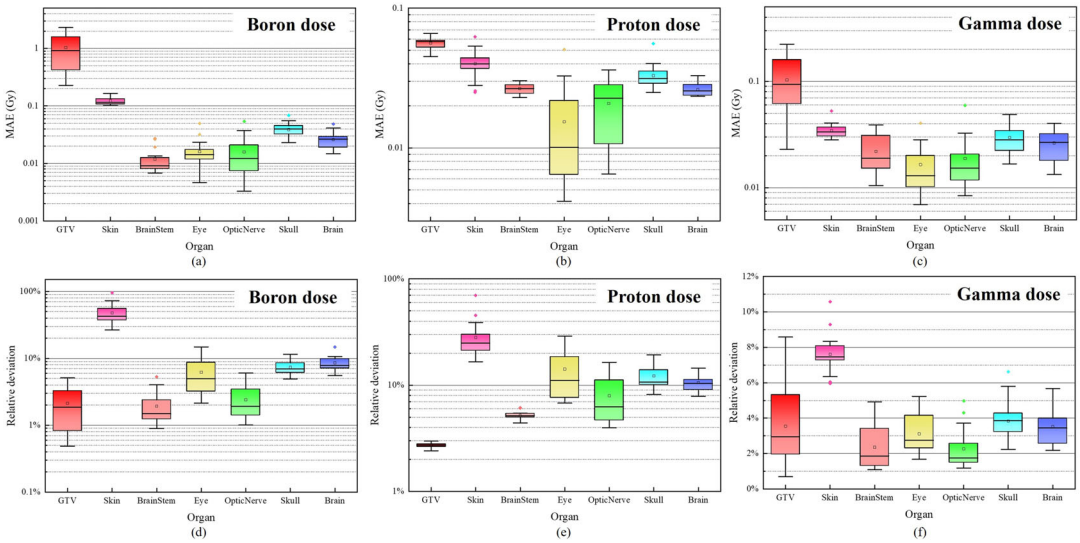

FIGURE 5 The MAE and relative deviation results of D_{NN} and D_{MC}. (a) MAE between D_{NN} and D_{MC} of boron dose. (b) MAE between D_{NN} and D_{MC} of proton dose. (c) MAE between D_{NN} and D_{MC} of gamma dose. (d) Relative deviation between D_{NN} and D_{MC} of boron dose. (e) Relative deviation between D_{NN} and D_{MC} of proton dose. (f) Relative deviation between D_{NN} and D_{MC} of gamma dose.

to analyze the reason, the skin pixels have been classified according to the simulated dose, and the mean relative deviation between D_{NN} and D_{MC} under each dose range have been calculated, as shown in Figure 6. It can be seen that the larger the dose deposited in the skin pixel, the smaller the relative deviation between the D_{NN} and D_{MC} in these pixels. Therefore, it can be explained that although the relative deviation between D_{NN} and D_{MC} of skin is large, these relative deviations are mainly generated by the pixels with the dose less than 1 Gy (or even lower), and it will not affect the accuracy of the 3D dose therapeutic prediction.

3.2 | Evaluation of predicted dose distribution based on DVH and gamma index

In addition to analyzing the dose values of each organ or voxel, we perform the DVH analysis for each patient with glioblastoma, and the results of four patients with glioblastoma are shown in Figure 7. The predicted DVH in different organs of patients with glioblastoma is basically consistent with the simulated DVH. Figure 8 shows the relative deviation results of dose received by D_{99}, D_{98}, D_{95}, D_{50}, and D_2 of all patients. The average deviation between the GTV doses of D_{99}, D_{98}, D_{95}, D_{50}, and D_2 are less than 2%, indicating that the predicted GTV dose distributions of different patients with glioblastoma in this work are consistent with the simulated GTV dose. Finally, for all test data, the average 2 mm/2% gamma index is 89.67% (85.20%, 94.14%), and the average 3 mm/3% gamma index is 96.78% (95.12%, 98.44%), and the values in parentheses represent 95% confidence intervals. There are, in fact, several cases which the performance of the 3D dose distribution predicted are not satisfactory, as shown in Figure 9. The GTV of patient 5 is almost closest to the body surface in all cases involved in this work, also the tumor is quite large, therefore these effects would deteriorate the performance of 3D dose prediction.

TABLE 2 Relative deviations between D_{NN} and D_{MC} of different organs

Organ	Relative deviation (%) (95% Confidence Interval)
GTV	2.097 (1.414, 2.779)
Skin	11.753 (10.711, 12.794)
Brain stem	1.868 (1.532, 2.205)
Eye	3.206 (2.528, 3.884)
Optic nerve	1.976 (1.566, 2.386)
Skull	3.578 (3.164, 3.992)
Brain	3.294 (2.844, 3.745)

4 | DISCUSSION

In this study, a novel method based on NN to predict the BNCT 3D dose distribution is proposed to solve the complex and time-consuming problems of dose calculation based on MC simulation. Compared with traditional photon radiotherapy, the neutron beam used in BNCT has a wide energy range, and the transport process of neutrons in biological tissues is complex. In addition, the dose components of BNCT are complex due to the complicated neutron reactions. These problems make the BNCT 3D therapeutic dose prediction difficult.

TABLE 3 Different doses obtained by MC simulation and NN prediction

	D_{max} (Gy) (95% Confidence Interval)	D_{mean} (Gy) (95% Confidence Interval)	D_{min} (Gy) (95% Confidence Interval)
GTV simulated	62.387 (61.170, 63.603)	53.791 (52.585, 54.998)	43.796 (41.475, 46.116)
GTV predicted	62.448 (61.240, 63.656)	54.039 (53.019, 55.059)	44.012 (41.973, 46.051)
Skin simulated	13.649 (13.251, 14.048)	2.050 (1.946, 2.154)	0.116 (0.103, 0.129)
Skin predicted	13.762 (13.405, 14.119)	1.987 (1.888, 2.085)	0.075 (0.066, 0.085)
Brain stem simulated	4.256 (3.900, 4.612)	2.343 (2.159, 2.527)	0.869 (0.792, 0.946)
Brain stem predicted	4.228 (3.880, 4.576)	2.347 (2.164, 2.530)	0.893 (0.816, 0.971)
Eye simulated	2.542 (1.729, 3.355)	1.145 (0.819, 1.471)	0.439 (0.367, 0.512)
Eye predicted	2.543 (1.737, 3.349)	1.152 (0.829, 1.476)	0.425 (0.354, 0.496)
Optic nerve simulated	2.915 (2.304, 3.526)	1.962 (1.529, 2.394)	1.140 (0.901, 1.379)
Optic nerve predicted	2.904 (2.303, 3.505)	1.964 (1.537, 2.391)	1.134 (0.905, 1.364)
Skull simulated	11.221 (10.917, 11.526)	2.633 (2.454, 2.811)	0.150 (0.124, 0.176)
Skull predicted	11.273 (10.983, 11.563)	2.655 (2.483, 2.826)	0.144 (0.123, 0.164)
Brain simulated	12.512 (12.176, 12.849)	2.547 (2.439, 2.655)	0.117 (0.105, 0.129)
Brain predicted	12.359 (12.058, 12.659)	2.542 (2.442, 2.642)	0.097 (0.083, 0.111)

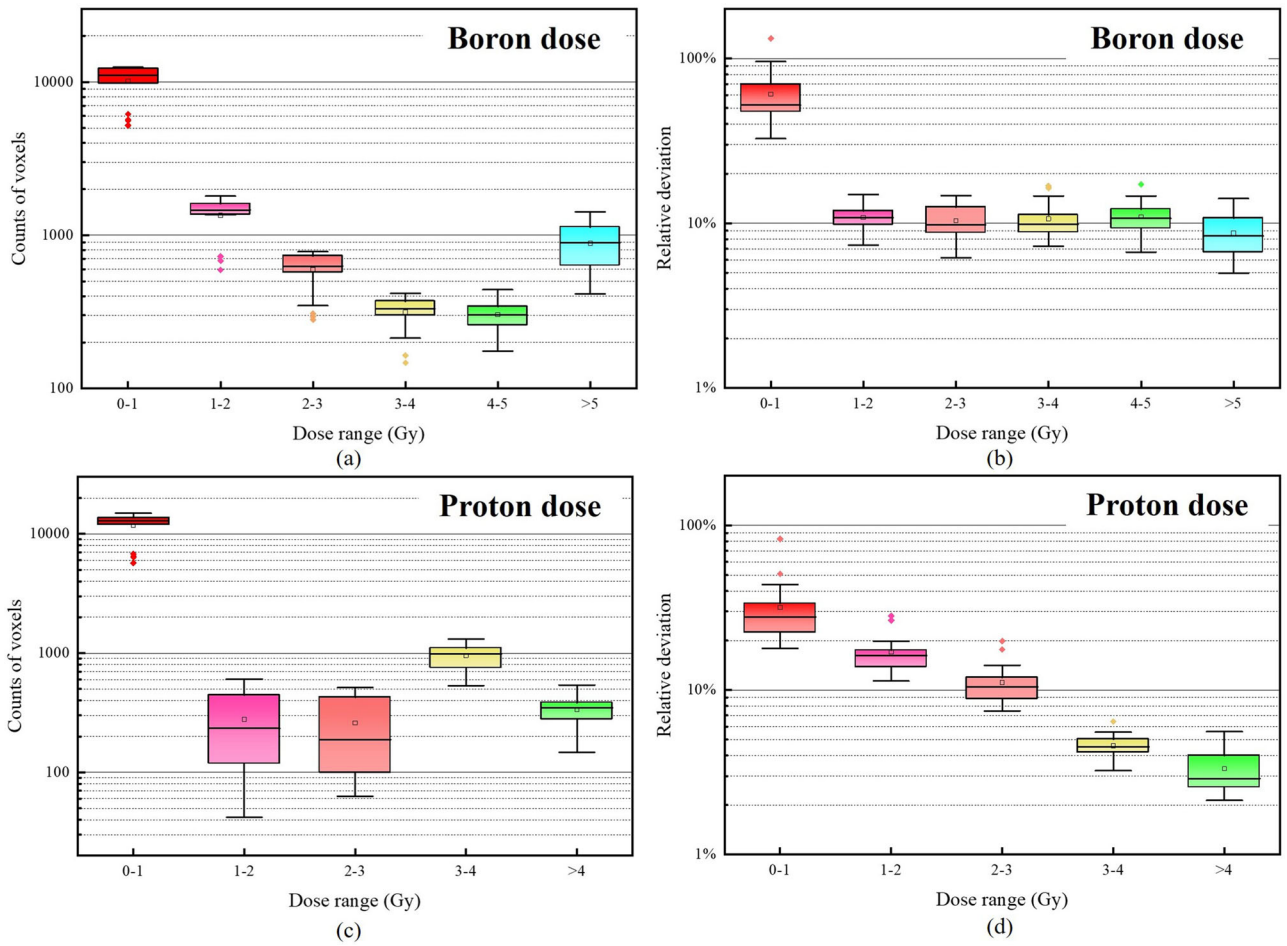

FIGURE 6 (a) Voxel counts under different boron dose range. (b) Relative deviation between D_{NN} and D_{MC} of boron dose under different dose range. (c) Voxel counts under different proton dose range. (d) Relative deviation between D_{NN} and D_{MC} of proton dose under different dose range.

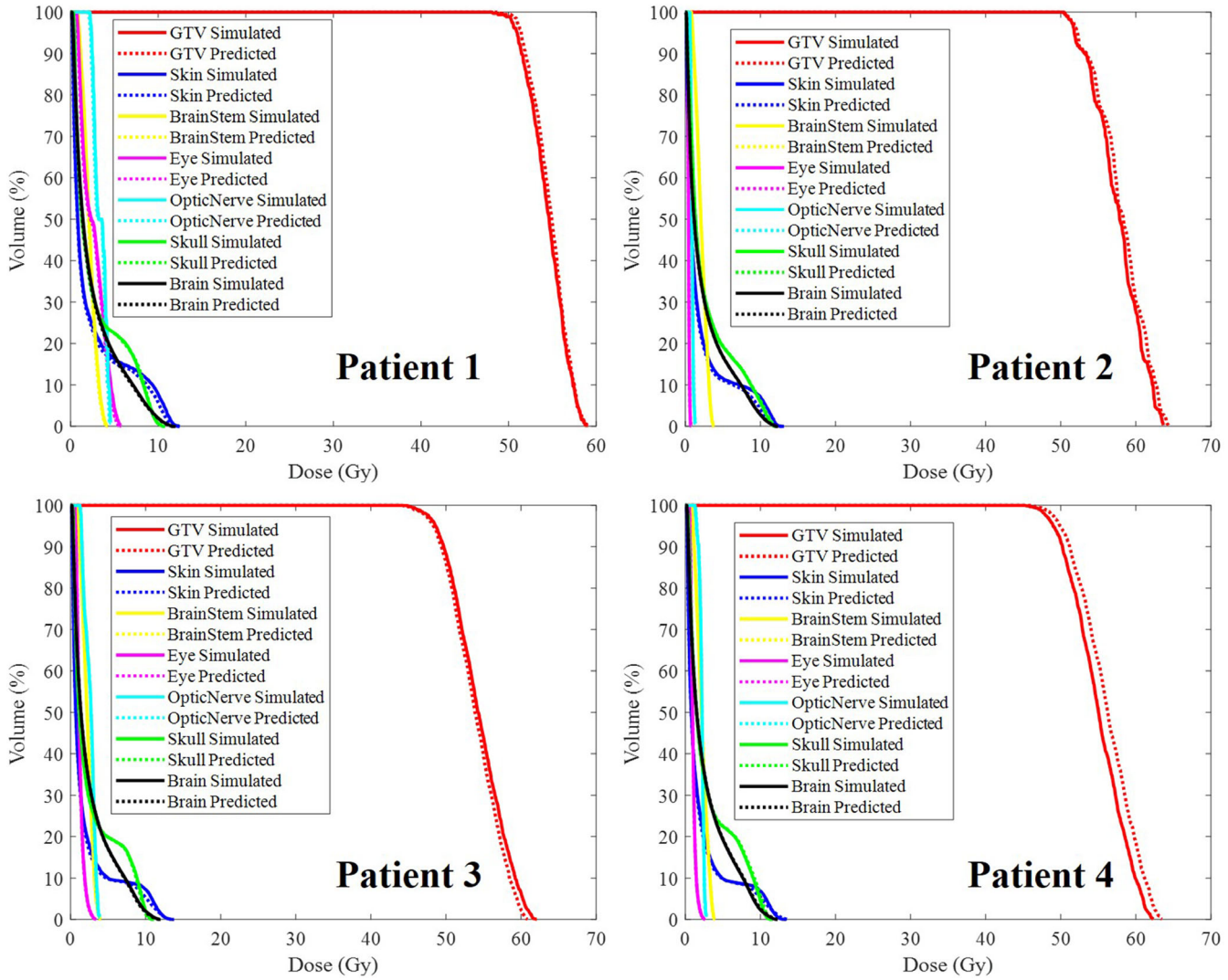

FIGURE 7 Examples of DVH comparison between simulated (solid line) and predicted (dashed line) results.

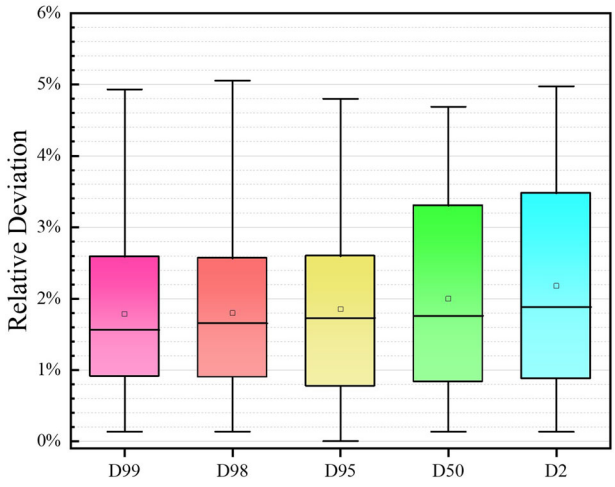

FIGURE 8 Average dose results for GTV in all tested glioblastoma patients.

Considering the physical principles behind the dose calculation, we designed four inputs for NN, that is, ① 3D density image; ② 3D irradiation field; ③ 3D patient contour; ④ a 3D image calculated by multiplying image ① and ②. We train three networks to achieve the prediction of different dose components. The purpose of inputting 3D density distribution to the 3D U-NET network is to enable the network for the analysis of the attenuation law of different radiation particles in the patient's body. BNCT generally adopts a fixed large irradiation field (i.e., the diameter is 12 cm), which will lead to large dose differences inside and outside the irradiation field. Therefore, the irradiation field information should be input. In addition, our previous experiments showed that the predicted image is blurred, specifically, the background area outside the patient body often has the dose value. To solve this problem, we input the contour of the patient body to the network. Finally, considering the strong attenuation of neutrons in tissue, the 3D density distribution image

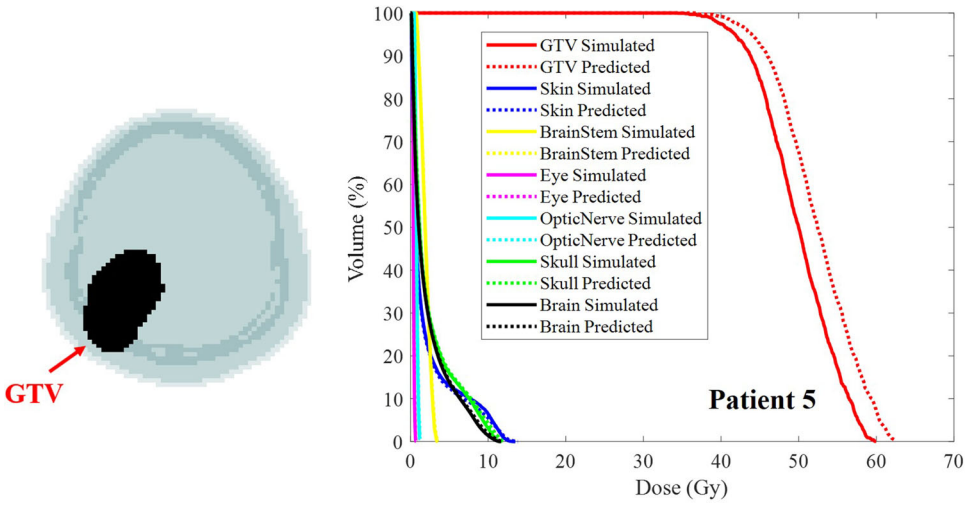

FIGURE 9 Cases with poor 3D dose distribution prediction results.

and the irradiation field image are combined as an input to strengthen the judgment of the network on the law of dose change with depth distribution.

Loss function results show that with the increase of training epochs, the three networks are eventually converging without overfitting, which means that the input and output samples designed in this study are reasonable. Further, the performance of dose prediction is evaluated through a series of evaluation methods. From the R_{dev} distribution between D_{NN} and D_{MC}, the voxels where the R_{dev} is large are mainly at the edge of the radiation field, that is the skin. According to the statistical results of the R_{dev} of different organs in all test cases, the R_{dev} of skin can reach more than 10%. This phenomenon may be caused by the steep drop in the dose value in the edge area and the fact that the boron concentration and biological effect factors in the skin are much higher than those in other normal tissues in BNCT. However, from the perspective of equivalent dose values in different organs, the average MAE between the D_{NN} and D_{MC} of skin is only about 0.2 Gy. This result proves that the dose deviation of the skin will not affect the application of this method. In addition to the skin area, we are more concerned about the dose prediction results in the GTV area. The average MAE of GTV is the largest of all organs, but the average MAE is only about 1 Gy. There is a certain deviation between the simulated and predicted DVH curves of the GTV, but the relative deviation from D_{99} to D_2 are all less than 2%, which indicates the accuracy of dose prediction in the GTV area. For all test data, the average 2 mm/2% gamma index is 89.67%, and the average 3 mm/3% gamma index is 96.78%, which indicate that the BNCT therapeutic dose prediction method based on NN proposed in this work has high accuracy.

The most important advantage of the BNCT dose prediction method is that it can remarkedly reduce the time for BNCT dose calculation. The dose results involved in this study are all simulated by the Intel Xeon(R) CPU E5-2699 v4. When using Intel Xeon E5-2699 v4 for Monte Carlo simulation, the average calculation time for each patient with glioblastoma is about 6 h. All training and testing are implemented on a NVIDIA 127 TITAN V 12GB graphics cards by using the deep learning framework Pytorch. The time required to train 250 epochs of each dose is about 1.5 h, whereas using the trained network to predict the 3D therapeutic dose for each patient with glioblastoma only takes about 1 s. In other words, the calculation speed of BNCT 3D dose distribution by the method proposed in this study is 21 600 times faster than the MC method, and this effect is also evidently better than other methods. For example, Lee et al. proposed a GPU-based MC method to calculate the BNCT dose, which can increase the calculation speed by 56 times.[17] Kotiluoto et al. developed a deterministic 3D radiation transport code MultiTrans SP_3, which can be over an order of magnitude faster than stochastic MC codes under the similar resolution.[40] These methods can reduce the 3D dose calculation time of BNCT to tens of minutes, but the 3D dose results can be predicted within a few seconds by the NN method proposed in this work.

This work demonstrates the feasibility of 3D BNCT therapeutic dose prediction method based on NN. We believe that this 3D therapeutic dose prediction method can be applied in many aspects of BNCT in the future. For example, this method can be used to evaluate quickly whether the patient is suitable for BNCT, assist the physicist to complete the formulation of BNCT treatment plan, or quickly evaluate the treatment effect during the treatment. Since this work only focuses on patients with glioblastoma and where the tumors' depth from the top of the head are less than 5 cm, some results also show that the 3D dose prediction performance of some special cases is not satisfactory due to insufficient

data samples. However, it should be noted that the BNCT 3D dose prediction method proposed in this paper is a universal method, which means that the method is still applicable to the prediction of 3D dose distribution of other tumors and also when using an accelerator-based neutron source. For different tumor cases, the input samples may need to be adjusted to realize the dose prediction. Therefore, more data samples with different tumors will be further added to establish 3D BNCT therapeutic dose prediction methods for different cases.

5 | CONCLUSION

In the clinical application of BNCT, the time-consuming problem of BNCT dose calculation based on MC simulation is not conducive to the rapid formulation of a BNCT treatment plan. In this paper, a novel 3D dose prediction method based on NN is proposed. The accurate prediction of 3D BNCT therapeutic dose distribution is realized through data set acquisition and network model construction. Results show that the average MAEs of the D_{NN} and D_{MC} of each organ are all less than 1 Gy, and the relative deviation of the predicted dose of GTV is less than 2%. DVH results show that the predicted dose distribution of each organ is basically consistent with the simulation results. The average 2 mm/2% gamma index is 89.67%, and the average 3 mm/3% gamma index is 96.78%. In addition, the time to obtain the 3D therapeutic dose distribution of different patients can be reduced from 6 h to almost 1 s. These results indicate that the 3D BNCT therapeutic dose prediction method based on NN proposed in this work can remarkably reduce the time required for calculation and ensure dose accuracy. The dose prediction method proposed in this work can be expected to promote significantly the clinical development of BNCT in the future.

ACKNOWLEDGMENTS

This work was supported by the National Key Research and Development Program (Grant No. 2022YFE0107800), the National Natural Science Foundation of China (Grant No. 12220101005), Natural Science Foundation of Jiangsu Province (Grant No. BK20220132), and the Fundamental Research Funds for the Central Universities (Grant No. NG2022004).

CONFLICT OF INTEREST

The authors have no relevant conflicts of interest to disclose.

REFERENCES

1. Suzuki M. Boron neutron capture therapy (BNCT): a unique role in radiotherapy with a view to entering the accelerator-based BNCT era. *Int J Clin Oncol*. 2020;25(1):43-50. doi:10.1007/s10147-019-01480-4
2. Moss RL. Critical review, with an optimistic outlook, on boron neutron capture therapy (BNCT). *Appl Radiat Isot*. 2014;88:2-11. doi:10.1016/j.apradiso.2013.11.109
3. Kawabata S, Suzuki M, Hirose K, et al. Accelerator-based BNCT for patients with recurrent glioblastoma: a multicenter phase II study. *Neuro-Oncol Adv*. 2021;3(1):vdab067. doi:10.1093/noajnl/vdab067
4. Sauerwein W, Moss R, Rassow J, et al. Organisation and management of the first clinical trial of BNCT in Europe (EORTC protocol 11961). *Strahlenther Onkol*. 1999;175(2):108-111. doi:10.1007/BF03038906
5. Joensuu H, Kankaanranta L, Seppälä T, et al. Boron neutron capture therapy of brain tumors: clinical trials at the Finnish facility using boronophenylalanine. *J Neurooncol*. 2003;62(1):123-134. doi:10.1007/BF02699939
6. Yong Z, Song Z, Zhou Y, et al. Boron neutron capture therapy for malignant melanoma: first clinical case report in China. *Chinese J Cancer Res*. 2016;28(6):634. 10.21147/j.issn.1000-9604.2016.06.10
7. Zhang X, Geng C, Tang X, et al. Assessment of long-term risks of secondary cancer in paediatric patients with brain tumours after boron neutron capture therapy. *J Radiol Prot*. 2019;39(3):838. doi:10.1088/1361-6498/ab29a3
8. Yamamoto T, Nakai K, Matsumura A. Boron neutron capture therapy for glioblastoma. *Cancer Lett*. 2008;262(2):143-152. doi:10.1016/j.canlet.2008.01.021
9. Barth RF, H Vicente M, Harling OK, et al. Current status of boron neutron capture therapy of high grade gliomas and recurrent head and neck cancer. *Radiat Oncol*. 2012;7(1):1-21. doi:10.1186/1748-717X-7-146
10. Cerullo N, Daquino G, Muzi L, Esposito J. Development of a treatment planning system for BNCT based on positron emission tomography data: preliminary results. *Nucl Instrum Methods Phys Res, Sect B*. 2004;213:637-640. doi:10.1016/S0168-583X(03)01668-9
11. Liu YH, Lee PY, Lin Y-C, et al. Dose estimation of animal experiments at the THOR BNCT beam by NCTPlan and Xplan. *Appl Radiat Isot*. 2014;88:125-128. doi:10.1016/j.apradiso.2014.01.032
12. Nigg D, Wemple C, Wessol D, et al. SERA–An advanced treatment planning system for neutron therapy and BNCT. *Trans Am Nucl Soc*. 1999;80(CONF-990605-).
13. Lin T-Y, Liu Y-WH. Development and verification of THORplan—a BNCT treatment planning system for THOR. *Appl Radiat Isot*. 2011;69(12):1878-1881. doi:10.1016/j.apradiso.2011.03.025
14. Hu N, Tanaka H, Kakino R, et al. Evaluation of a treatment planning system developed for clinical boron neutron capture therapy and validation against an independent Monte Carlo dose calculation system. *Radiat Oncol*. 2021;16(1):1-13. doi:10.1186/s13014-021-01968-2
15. Kumada H, Yamamoto K, Matsumura A, Yamamoto T, Nakagawa Y, Development of JCDS, a computational dosimetry system at JAEA for boron neutron capture therapy. Paper presented at: J Phys: conference series2007. doi:10.1088/1742-6596/74/1/021010
16. Chen J, Teng Y-C, Zhong W-B, Yang H-B, Hong Q, Liu Y-H, Development of Monte Carlo based treatment planning system for BNCT. Paper presented at: J Phys: Conference Series2022. doi:10.1088/1742-6596/2313/1/012012
17. Lee C-M, Lee H-S. Development of a dose estimation code for BNCT with GPU accelerated Monte Carlo and collapsed cone convolution method. *Nucl Eng Technol*. 2022;54(5):1769-1780. doi:10.1016/j.net.2021.11.010
18. Sahiner B, Pezeshk A, Hadjiiski LM, et al. Deep learning in medical imaging and radiation therapy. *Med Phys*. 2019;46(1):e1-e36. doi:10.1002/mp.13264

19. Boldrini L, Bibault J-E, Masciocchi C, Shen Y, Bittner M-I. Deep learning: a review for the radiation oncologist. *Front Oncol*. 2019;9:977. doi:10.3389/fonc.2019.00977
20. Mahesh B. Machine learning algorithms-a review. *Int J Sci Res (IJSR)*. 2020;9:381-386.
21. Shao Y, Zhang X, Wu G, et al. Prediction of three-dimensional radiotherapy optimal dose distributions for lung cancer patients with asymmetric network. *IEEE J Biomed Health Inform*. 2020;25(4):1120-1127. doi:10.1109/JBHI.2020.3025712
22. Fan J, Wang J, Chen Z, Hu C, Zhang Z, Hu W. Automatic treatment planning based on three-dimensional dose distribution predicted from deep learning technique. *Med Phys*. 2019;46(1):370-381. doi:10.1002/mp.13271
23. Ahangari R, Afarideh H. A new approach to dose estimation and in-phantom figure of merit measurement in BNCT by using artificial neural networks. *Australas Phys Eng Sci Med*. 2011;34(4):467-479. doi:10.1007/s13246-011-0107-z
24. Falk T, Mai D, Bensch R, et al. U-Net: deep learning for cell counting, detection, and morphometry. *Nat Methods*. 2019;16(1):67-70. doi:10.1038/s41592-018-0261-2
25. Çiçek Ö, Abdulkadir A, Lienkamp SS, Brox T, Ronneberger O, 3D U-Net: learning dense volumetric segmentation from sparse annotation. Paper presented at: International conference on medical image computing and computer-assisted intervention2016. doi:10.1007/978-3-319-46723-8_49
26. Ronneberger O, Fischer P, Brox T, U-net: convolutional networks for biomedical image segmentation. Paper presented at: International Conference on Medical image computing and computer-assisted intervention 2015. doi:10.1007/978-3-319-24574-4_28
27. Simonyan K, Zisserman A. *Very deep convolutional networks for large-scale image recognition*. arXiv preprint arXiv; 2014:14091556. 10.48550/arXiv.1409.1556
28. Xu B, Wang N, Chen T, Li M. *Empirical evaluation of rectified activations in convolutional network*. arXiv preprint arXiv; 2015:150500853. 10.48550/arXiv.1505.00853
29. Ishiyama S. Deterministic parsing model of the compound biological effectiveness (CBE) factor for intracellular 10 boron distribution in boron neutron capture therapy. *J Cancer Ther*. 2014;5(14):1388. doi:10.4236/jct.2014.514140
30. Aihara T, Hiratsuka J, Morita N, et al. First clinical case of boron neutron capture therapy for head and neck malignancies using 18F-BPA PET. *Head Neck*. 2006;28(9):850-855. doi:10.1002/hed.20418
31. Nichols TL, Kabalka GW, Miller LF, Khan MK, Smith GT. Improved treatment planning for boron neutron capture therapy for glioblastoma multiforme using fluorine-18 labeled boronophenylalanine and positron emission tomography. *Med Phys*. 2002;29(10):2351-2358. doi:10.1118/1.1507780
32. Zhao S, Geng C, Guo C, Tian F, Tang X. SARU: a self-attention ResUNet to generate synthetic CT images for MR-only BNCT treatment planning. *Med Phys*. 2023;50(1):117-127. doi:10.1002/mp.15986
33. Fukuda H, Hiratsuka J. Pharmacokinetics of 10B-p-boronophenylalanine (BPA) in the blood and tumors in human patients: a critical review with special reference to tumor-to-blood (T/B) ratios using resected tumor samples. *Appl Radiat Isot*. 2020;166:109308. doi:10.1016/j.apradiso.2020.109308
34. Fukuda H. Response of normal tissues to boron neutron capture therapy (BNCT) with 10B-borocaptate sodium (BSH) and 10B-Paraboronophenylalanine (BPA). *Cells*. 2021;10(11):2883. doi:10.3390/cells10112883
35. Kiger W III, Sakamoto S, Harling O. Neutronic design of a fission converter-based epithermal neutron beam for neutron capture therapy. *Nucl Sci Eng*. 1999;131(1):1-22. 10.13182/NSE99-A2015
36. Tian F, Geng C-R, Tang X-B, et al. Analysis of influencing factors on the method for determining boron concentration and dose through dual prompt gamma detection. *Nucl Sci Tech*. 2021;32(4):1-10. doi:10.1007/s41365-021-00873-3
37. Liu Z, Chen J. New calculations of neutron kerma coefficients and dose equivalent. *J Radiol Prot*. 2008;28(2):185. doi:10.1088/0952-4746/28/2/002
38. Wendling M, Zijp LJ, McDermott LN, et al. A fast algorithm for gamma evaluation in 3D. *Med Phys*. 2007;34(5):1647-1654. doi:10.1118/1.2721657
39. Brownlee J. What is the difference between a batch and an epoch in a neural network. *Mach Learn Mastery*. 2018:20. https://deeplearning.lipingyang.org/wp-content/uploads/2018/07/What-is-the-Difference-Between-a-Batch-and-an-Epoch-in-a-Neural-Network_.pdf
40. Kotiluoto P, Hiismäki P, Savolainen S. Application of the new MultiTrans radiation transport code in BNCT dose planning. *Med Phys*. 2001;28(9):1905-1910. doi:10.1118/1.1397716

SUPPORTING INFORMATION

Additional supporting information can be found online in the Supporting Information section at the end of this article.

How to cite this article: Tian F, Zhao S, Geng C, Guo C, Wu R, Tang X. Use of a neural network-based prediction method to calculate the therapeutic dose in boron neutron capture therapy of patients with glioblastoma. *Med Phys*. 2023;50:3008–3018. https://doi.org/10.1002/mp.16215